QUANTUM NATURE OF CYCLOTRON HARMONICS IN THERMAL SPECTRA OF NEUTRON STARS

V. F. Suleimanov[1,2], G. G. Pavlov[3], and K. Werner[1]

ABSTRACT

Some isolated neutron stars show harmonically spaced absorption features in their thermal soft X-ray spectra. The interpretation of the features as a cyclotron line and its harmonics has been suggested, but the usual explanation of the harmonics as caused by relativistic effects fails because the relativistic corrections are extremely small in this case. We suggest that the features correspond to the peaks in the energy dependence of the free-free opacity in a quantizing magnetic field, known as quantum oscillations. The peaks arise when the transitions to new Landau levels become allowed with increasing the photon energy; they are strongly enhanced by the square-root singularities in the phase-space density of quantum states in the case when the free (non-quantized) motion is effectively one-dimensional. To explore observable properties of these quantum oscillations, we calculate models of hydrogen neutron star atmospheres with $B \sim 10^{10}$–10^{11} G (i.e., electron cyclotron energy $E_{c,e} \sim 0.1$–1 keV) and $T_{\rm eff} = 1$–3 MK. Such conditions are thought to be typical for the so-called central compact objects in supernova remnants, such as $1E\,1207.4$–5209 in PKS 1209–51/52. We show that observable features at the electron cyclotron harmonics form at moderately large values of the quantization parameter, $b_{\rm eff} \equiv E_{c,e}/kT_{\rm eff} \simeq 0.5$–$20$. The equivalent widths of the features can reach ~ 100–200 eV; they grow with increasing $b_{\rm eff}$ and are lower for higher harmonics.

Subject headings: radiative transfer — stars: neutron — stars: magnetic fields — pulsars: individual (1E 1207.4-5209, PSR J1210–5226, PSR J1852+0040, PSR J0821–4300)

1. INTRODUCTION

Observations with the X-ray observatories *Chandra* and *XMM-Newton* have led to the discovery of absorption features in the thermal spectra of several isolated (nonaccreting) neutron stars (NSs). Studying such features, one could infer the chemical composition, magnetic field, and gravitational redshift at the NS surface, but identification of the features is rather complicated, mostly because of the effects of the a priori unknown NS magnetic field on radiative transitions in the X-ray range.

First absorption features in the spectrum of an isolated NS, centered at about 0.7 and 1.4 keV, were discovered by Sanwal et al. (2002) in *Chandra* observations of 1E 1207.4–5209 (hereafter 1E 1207), which is the central compact object (CCO) of the supernova remnant (SNR) PKS 1209–51/52. Similar to other CCOs (Pavlov et al. 2002, 2004; de Luca 2008; Halpern & Gotthelf 2010), 1E 1207 does not show the usual pulsar activity, such as radio and γ-ray emission or a pulsar wind nebula. This NS has the period $P = 0.424$ s (Zavlin et al. 2000) and shows a thermal-like X-ray spectrum ($T_{\rm eff} \sim 1$–3 MK, depending on the model; Zavlin et al. 1998). Further observations with *XMM-Newton* suggested the presence of two more features, at 2.1 and 2.8 keV (Bignami et al. 2003).

As the energies of the spectral features are harmonically spaced, it seems natural to interpret them as

[1] Institute for Astronomy and Astrophysics, Kepler Center for Astro and Particle Physics, Eberhard Karls University, Sand 1, 72076 Tübingen, Germany; suleimanov@astro.uni-tuebingen.de
[2] Dept. of Astronomy, Kazan State University, Kremlevskaya 18, 420008 Kazan, Russia
[3] Pennsylvania State University, 525 Davey Lab., University Park, PA 16802; pavlov@astro.psu.edu

(gravitationally redshifted) electron cyclotron line and its harmonics (e.g., due to the "resonance cyclotron scattering", by analogy with accreting X-ray pulsars; Bignami et al. 2003), formed in the magnetic field $B = 6 \times 10^{10}(E_{c,e}^{\infty}/0.7\,{\rm keV})(1+z)$ G, where $E_{c,e}^{\infty}(1+z) = E_{c,e} = \hbar eB/m_e c$ is the electron cyclotron energy, and z is the gravitational redshift. This estimate for the magnetic field is consistent with the upper limit $B_{sd} < 3.3 \times 10^{11}$ G obtained by Gotthelf & Halpern (2007) from the upper limit on the pulsar's period derivative $\dot{P}$.

However, the cyclotron harmonic interpretation encounters a serious problem because the ratio of the emissivities (or oscillator strengths) of consecutive harmonics is known to be proportional to the parameter $\xi_e \equiv \max(kT, E_{c,e})/m_e c^2$ (see, e.g., Pavlov et al. 1980a,b), i.e., the emission and absorption in cyclotron harmonics is an essentially relativistic phenomenon. As this parameter is quite small for 1E 1207, $\xi_e \sim 10^{-3}$, observable cyclotron harmonics can hardly be expected, even with allowance for the fact that the strength of a feature formed in an optically thick medium depends on the oscillator strength nonlinearly, and it also depends on other factors, such as the temperature gradient at the depth where the feature is formed. We should note that the conditions in the relatively cold, low-field atmospheres of 1E 1207 and other CCOs (where the free-free absorption and emission dominate over the electron scattering of photons) are quite different from those in accreting X-ray pulsars, where the parameter ξ_e is a factor of 30–100 larger, which explains the observability of electron cyclotron harmonics in those objects (e.g., two harmonics, in addition to the fundamental at 26 keV, have been observed in the binary pulsar V0332+53; Pottschmidt et al. 2005) .

Resonances at cyclotron harmonics (also known as quantum oscillations) can, however, arise even in a non-

relativistic plasma due to quantization of rotation of a charged particle in a magnetic field. In particular, the energy of, e.g., a nonrelativistic electron is

$$\epsilon_n(p_z) = \left(n + \frac{1}{2}\right) E_{c,e} + \frac{p_z^2}{2m_e}, \qquad (1)$$

where $n = 0, 1, 2, \ldots$ numerates the Landau levels, and p_z is the (continuous) electron's momentum along the magnetic field. As a result of the quantization, various properties of matter show discontinuities when the number of the involved Landau levels changes (e.g., when a transition to a higher Landau level becomes allowed with increasing the energy of the photon that causes this transition). Moreover, because the electron motion is continuous only in one dimension, the phase space density of final electron states in such transitions experiences square-root singularities at these discontinuities, which gives rise to logarithmically high resonances at harmonics of the cyclotron energy (see Section 2 for more detail).

Such quantum resonances in free-free absorption of photons in a magnetic field were first noticed by Pavlov & Panov (1976; hereafter PP76) who derived the spectral opacities and emissivities of a plasma with $kT \ll m_e c^2$ for different photon polarizations. As the free-free transitions are an important source of opacity in NS atmospheres, one can expect the resonances to manifest themselves as absorption spectral features in thermal spectra of NSs. This was qualitatively demonstrated by Pavlov & Shibanov (1978) who considered emission from an "atmosphere" in which the source function in the radiative transfer equation was approximated by a linear function of optical depth. More realistic, self-consistent NS atmosphere models have been developed later, starting from Shibanov et al. (1992), but they used approximate formulae for the free-free opacity, in which the quantum resonances were neglected.

Here we present first calculations of realistic magnetized NS atmosphere models with the quantum resonances at electron cyclotron harmonics in the free-free opacity taken into consideration and show that harmonically spaced absorption features are significant in the emergent spectra. These calculations demonstrate that thermal spectra of NSs with a surface magnetic field $\sim 10^{10}$–10^{11} G can exhibit several such features in the observable X-ray range, and, in particular, the features observed in the spectrum of 1E1207 can be interpreted as due to the quantum effects.

2. QUANTUM OSCILLATIONS OF OPACITIES

We consider hydrogen NS atmospheres with magnetic fields $\sim 10^{10}$–10^{11} G, such that the electron cyclotron energy, $E_{c,e} \sim 0.1$–1 keV, and its first several harmonics are in the soft X-ray range, observable with *Chandra* and *XMM-Newton*. We assume that the atmosphere is hot enough, $T_{\rm eff} \gtrsim 10^6$ K, to neglect the small fraction of neutral atoms. The opacity in such a fully ionized atmosphere is determined by two processes: free-free absorption (inverse bremsstrahlung) and scattering of photons by electrons[4], modified by the magnetic field. We assume that the atmosphere is cold enough, $T_{\rm eff} \lesssim 10^7$ K,

---

[4] Scattering by protons, as well as the proton contribution into the free-free absorption, can be neglected at the relatively low magnetic fields, when $E_{c,p} \ll E$.

to neglect the change of photon energy in the scattering process (comptonization effects). Moreover, we calculate the opacities in the so-called "cold plasma approximation" (Ginzburg 1970), which implies that relativistic effects, such as the cyclotron emission (hence also absorption and scattering) at the harmonics of the electron cyclotron energy, can be neglected, as well as the thermal motion effects, including the Doppler broadening of the cyclotron resonance.

The transfer of high energy radiation in a magnetized plasma is described by two coupled transfer equations for the ordinary and extraordinary normal modes (Gnedin & Pavlov 1974). The normal mode polarizations and opacities depend not only on the photon energy E but also on the angle θ_B between the wave vector and the magnetic field; they can be written as (e.g., Pavlov et al. 1995)

$$k_{1,2} = \sum_{\alpha=-1}^{+1} \frac{E^2}{(E + \alpha E_{c,e})^2 + (\gamma_r + \gamma_\alpha)^2} \times \qquad (2)$$

$$\left[k_{\rm T} + k_{\rm cl}^{\rm ff}(E) g_\alpha(E)\right] |e_\alpha^{1,2}(E, \theta_{\rm B})|^2,$$

where $k_{\rm cl}^{\rm ff}(E)$ and $k_{\rm T}$ are the "classical" free-free and Thomson opacities at $B = 0$, $g_{\pm 1}(E) = g_\perp(E)$ and $g_0 = g_\parallel(E)$ are the Gaunt factors for radiation polarized across and along the magnetic field, $\gamma_r = (2/3)E^2(e^2/\hbar m_e c^3)$ and $\gamma_\alpha = \gamma_r \left[k_{\rm cl}^{\rm ff}(E)/k_{\rm T}\right] g_\alpha(E)$ are the radiative and collisional widths, and $e_\alpha^{1,2}(E, \theta_B)$ are the projections of the normal mode polarization vectors (see Kaminker et al. 1982, 1983 for a detailed description of the normal mode polarizations and opacities in the cold plasma approximation).

Various forms for the magnetic Gaunt factors $g_{\perp,\parallel}(E)$ were derived by PP76[5] who calculated the dependence of the Gaunt factors on the dimensionless photon energy $x = E/kT$ for several values of the "quantization parameter" $b_e = E_{c,e}/kT$ and obtained simple expressions for limiting cases. Examples of the energy dependence of the Gaunt factors are shown in Figure 1, for $b_e = 5$, 0.05, and 0. In our calculations we used Equations (30) and (31) from PP76,

$$g_\parallel = \frac{3\sqrt{3}}{2\pi} b_e^{1/2} e^{x/2} \int_0^\infty \cos xt \times \qquad (3)$$

$$\left[\frac{\sqrt{A}}{A - D} - \frac{D}{(A - D)^{3/2}} \ln \frac{A^{1/2} + (A - D)^{1/2}}{D^{1/2}}\right] dt,$$

$$g_\perp = \frac{3\sqrt{3}}{4\pi} b_e^{1/2} e^{x/2} \int_0^\infty \cos xt \times \qquad (4)$$

$$\left[-\frac{\sqrt{A}}{A - D} + \frac{2A - D}{(A - D)^{3/2}} \ln \frac{A^{1/2} + (A - D)^{1/2}}{D^{1/2}}\right] dt,$$

where

$$A = b_e \left(t^2 + \frac{1}{4}\right), \qquad (5)$$

$$D = \coth \frac{b_e}{2} - \frac{\cos(b_e t)}{\sinh(b_e/2)} + \frac{m_e}{m_p} \left(t^2 + \frac{1}{4}\right).$$

---

[5] PP76 used Coulomb logarithms, $\Lambda_{\perp,\parallel} = (\pi/\sqrt{3}) g_{\perp,\parallel}$, instead of the Gaunt factors.

Figure 1 demonstrates that the energy dependences of the magnetic Gaunt factors oscillate around the smooth non-magnetic curve, with maxima at the cyclotron energy and its harmonics. The oscillations are strong in $g_\perp(E)$, especially at larger values of b_e, being almost imperceptible in $g_\parallel(E)$. If the last term in D is omitted (i.e., terms $\propto m_e/m_p$ are neglected), the cyclotron resonances in $g_\perp(E)$ diverge logarithmically (PP76; see the dashed curves in the upper panel of Figure 1). The origin of the oscillations and divergences can be understood as follows.

For an electron transition $n, p_z \to n', p_z'$ with absorption of a photon with energy E, the conservation of energy is described by the delta-function:

$$\delta\left[\frac{p_z'^2 - p_z^2}{2m_e} + sE_{c,e} - E\right] \qquad (6)$$

$$= \frac{m_e}{P}[\delta(p_z' - P) + \delta(p_z' + P)]\,\Theta(P^2),$$

where $P = [2m_e(E - sE_{c,e} + p_z^2/2m_e)]^{1/2}$, $s = n' - n$, and $\Theta(P^2) = \Theta(E - sE_{c,e} + p_z^2/2m_e)$ is the unit step function. The equation for the transition rate contains integrations over p_z' and p_z and summations over n and n' (or over n and s). Because of the step function in Equation (6), a new term in the sum over s is added whenever the increasing E passes through $kE_{c,e} - p_z^2/2m_e$ ($k = 1, 2, \ldots$). Each of the added terms contains a singular factor $\propto (E - kE_{c,e} + p_z^2/2m_e)^{-1/2}$ at $E \to kE_{c,e} - p_z^2/2m_e + 0$. Further averaging over p_z with the one-dimensional electron distribution function turns the square-root singularities into logarithmic singularities, $\propto \ln|E - kE_{c,e}|^{-1}$. Such behavior is seen in $g_\perp(E)$ but not in $g_\parallel(E)$ because in $g_\parallel(E)$ the singularity is canceled by the zero of the square of the transition matrix element for the longitudinal polarization $[\propto (p_z' - p_z)^2$; see Equations (20) and (26) in PP76].

There exist a number of mechanisms that broaden the peaks $E = kE_{c,e}$ and remove the logarithmic singularities (PP76). The last term in D (Equation [5]) accounts for one of such mechanisms, associated with the proton recoil (the broadened peaks of finite heights are shown by solid lines in Figure 1). When the magnetic field decreases, the distances between the peaks eventually become smaller than their widths, the oscillations disappear, and the magnetic Gaunt factors turn into the Gaunt factor at $B = 0$.

We emphasize that the oscillations in $g_{\perp,\parallel}(E)$ are solely due to quantization of the electron motion across the magnetic field, because of which the motion in only one dimension (along the magnetic field) remains nonquantized and the square-root singularities appear after the integration over the final longitudinal momentum p_z' (see Equation [6]). At $B \to 0$, when the quantization disappears, the integration over the final (three-dimensional) momentum with allowance for the energy conservation, $\int \ldots \delta[(p'^2 - p^2)/2m_e - E]\, d^3p' = 4\pi m_e P \int \ldots dp'$ [where p' and p are the moduli of the final and initial momentum vectors, and $P = (p^2 + 2m_e E)^{1/2}$], does not lead to singularities or oscillations.

3. ATMOSPHERE MODELS

To calculate the magnetic NS hydrogen atmosphere models, we use our recently developed code (Suleimanov et al. 2009), assuming the magnetic field
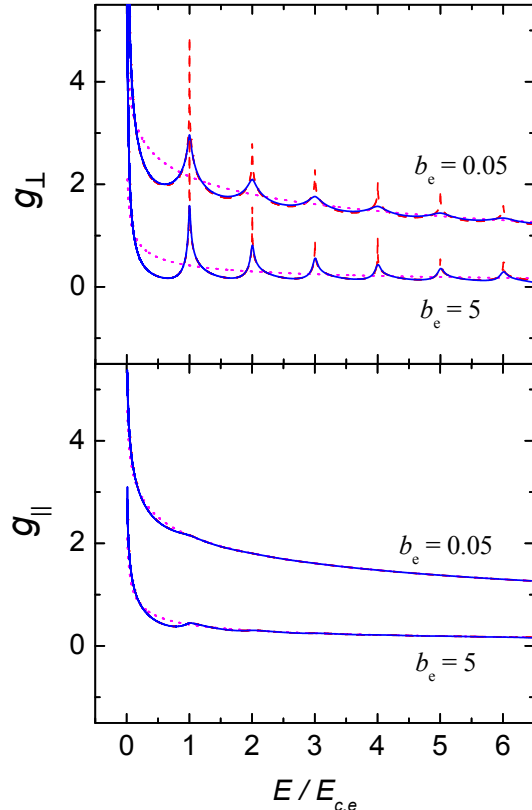

Figure 1. Dependence of the transverse and longitudinal Gaunt factors on relative photon energy for an electron-proton plasma with $b_e \equiv E_{c,e}/kT = 5$ and 0.05. The solid curves show the Gaunt factors with proton motion and recoil taken into account, the dashed curves show the Gaunt factors in the limit of $m_p \to \infty$, and the dotted curves are the Gaunt factors at $B = 0$.

normal to the stellar surface. We assume full ionization and neglect the vacuum polarization by the magnetic field because relatively weak magnetic fields are considered. For the opacities, we use the equations by van Adelsberg & Lai (2006), substituting there the above-described magnetic Gaunt factors[6]; these equations reduce to Equation (2) when the proton contribution is negligible.

Assuming the surface gravitational acceleration of 1×10^{14} cm s^{-2}, we calculated two sets of the atmosphere models. In the first set the magnetic field strength was fixed ($B = 7 \times 10^{10}$ G) and models with three different effective temperatures ($T_{\rm eff} = 1$, 1.5 and 3 MK) were constructed. A common property of the emergent spectra, as shown in Figure 2 (top panel), is prominent absorption features at the cyclotron energy and its harmonics, $E_k = kE_{c,e} = 0.81k$ keV ($k = 1, 2, \ldots$), which originate from the quantum peaks in $g_\perp(E)$. The equivalent width W_k of the k-th feature decreases with increasing k (similar to the strengths of the quantum peaks in the transverse Gaunt factor) as well as with increasing $T_{\rm eff}$ (i.e., with decreasing the effective quantization parameter, $b_{\rm eff} \equiv E_{c,e}/kT_{\rm eff} \approx 9.4, 6.3, 3.1$ for the three models). For instance, $W_1 = 240$, 200 and 180 eV at $T_{\rm eff} = 1$, 1.5 and 3 MK, respectively, while $W_2 = 190$, 140 and 55 eV

[6] van Adelsberg & Lai (2006) use the magnetic Gaunt factors by Nagel (1980), which are applicable only at $kT \ll E_{c,e}$ and $E < E_{c,e} - O(kT)$ (see the Appendix in Kaminker et al. 1983).
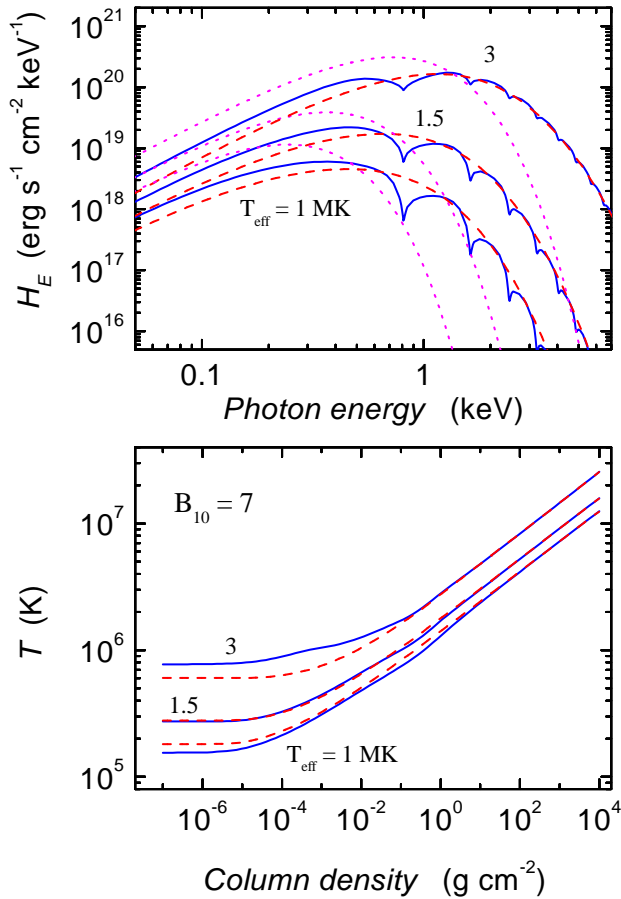
Figure 2. Emergent spectra (*top*) and temperature structures (*bottom*) for NS atmospheres with the magnetic field $B = 7 \times 10^{10}$ G (solid curves) and $B = 0$ (dashed curves) for three effective temperatures, $T_{\rm eff} = 1$, 1.5, and 3 MK. The dotted curves in the top panel show the blackbody spectra for the same temperatures.

Figure 3. *Top panel:* Emergent spectra for magnetic NS atmospheres with $T_{\rm eff} = 1.5$ MK and different magnetic fields ($B = 1$, 4, 7 and 10 $\times 10^{10}$ G), calculated with magnetic and non-magnetic Gaunt factors. For clarity, the spectra for $B_{10} = 10$, 7 and 1 are shifted along the ordinate axis by factors 10^{+1}, $10^{+0.5}$ and $10^{-0.5}$. *Bottom panel:* Temperature structures of the models with different magnetic fields: 1 (dash-dotted curve), 4 (dashed curve), 7 (solid curve), and 10 $\times 10^{10}$ G (dotted curve).

at the same temperatures.

In the top panel of Figure 2 we also show the emergent spectra for non-magnetic atmosphere models with the same effective temperatures. These spectra are close to the "continua" of the corresponding magnetic spectra at energies higher than the cyclotron energy, but they lie below the magnetic spectra at lower energies as the radiation emerges from deeper and hotter layers in the magnetic case because of lower opacities at $E \ll E_{c,e}$.

The second set consists of four models with different magnetic field strengths ($B = 1$, 4, 7, and 10 $\times 10^{10}$ G) at the same effective temperature ($T_{\rm eff} = 1.5$ MK). The emergent spectra are shown in the top panel of Figure 3. Again, the equivalent widths of the absorption features decrease with increasing harmonic number k and decreasing effective quantization parameter ($b_{\rm eff} = 0.9$, 3.6, 6.3 and 9.0 for the four models).

The radiation spectra in the ordinary (O) and extraordinary (X) polarization modes are shown in the top panel of Figure 4, together with the total (X+O) spectrum, for the model with $T_{\rm eff} = 1.5$ MK and $B = 7 \times 10^{10}$ G. As the X-mode opacity is low at $E \ll E_{c,e}$ due to the factor $E^2/[(E \pm E_{c,e})^2 + \gamma^2] \approx (E/E_{c,e})^2 \ll 1$, the X-mode radiation emerges from deep, hot layers and dominates at these energies. But at the cyclotron resonance the opacity in the X-mode is strongly increased, and the total
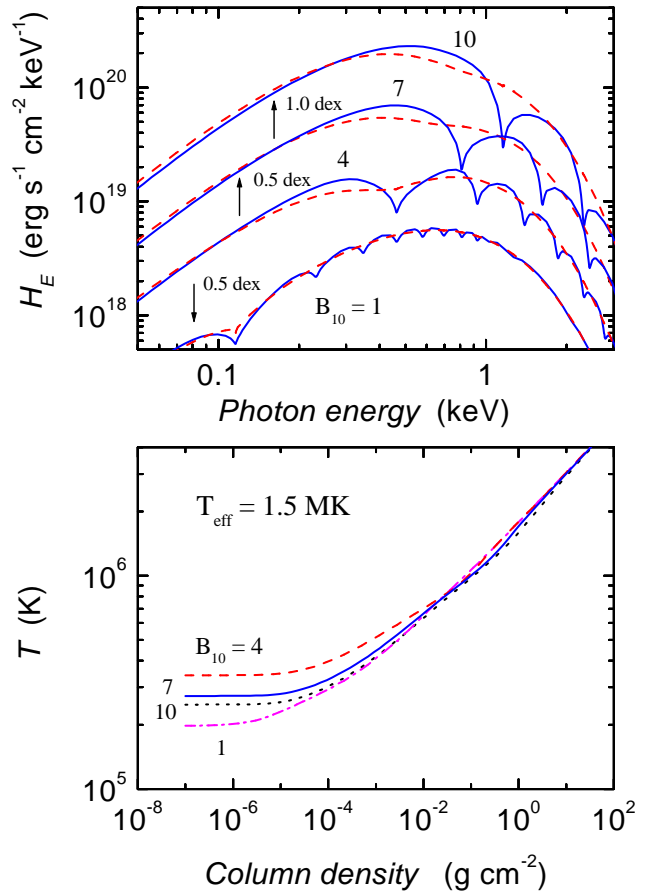
spectrum is mainly determined by the O-mode, whose opacity is about the same as at $B = 0$. As a result, the cyclotron absorption feature is very strong in the X-mode spectrum but not in the total spectrum because the X-mode flux is small (Pavlov & Shibanov 1978). This explains the lack of a strong cyclotron feature in the atmosphere spectra calculated with the non-magnetic Gaunt factors (see Figure 3, top panel). Instead of a strong absorption line, we see in these spectra a broad, shallow depression at $E \lesssim E_{c,e}$ (in the red wing of the cyclotron line), where the X-mode starts to dominate in the emergent spectrum. In contrast, the transverse Gaunt factor is present in the opacities of both modes, so that the corresponding absorption features are prominent in the outgoing spectrum.

Spectra of emergent specific intensity for the model with $T_{\rm eff} = 1.5$ MK and $B = 7 \times 10^{10}$ G for various angles θ between the line of sight and the surface normal are shown in the bottom panel of Figure 4. The quantum oscillations in the intensity spectra are seen at any angle; the equivalent width of the corresponding absorption features depends on θ nonmonotonously (e.g., $W_1 \simeq 220$, 160, 320 and 330 eV for $\theta = 1°$, 30°, 60° and
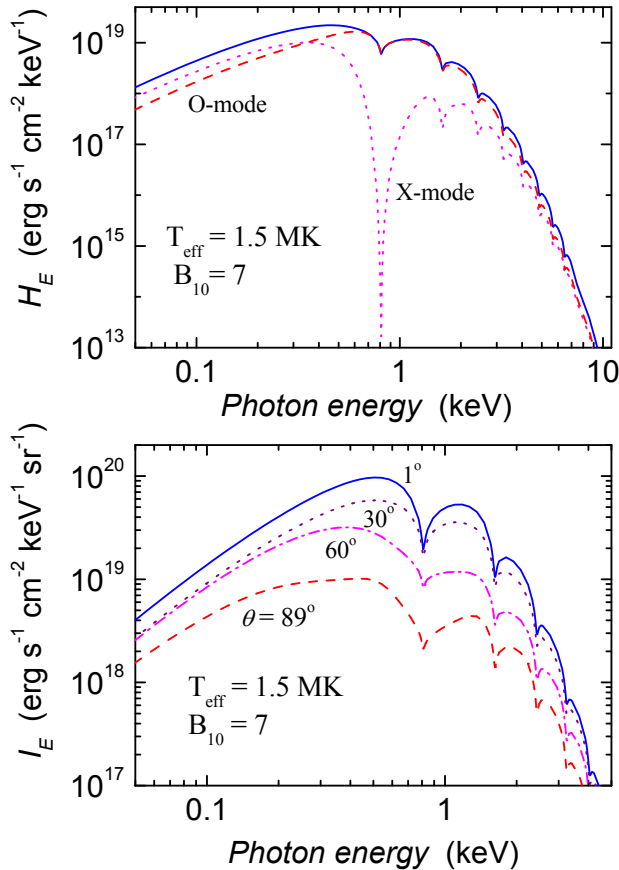
Figure 4. *Top panel:* Emergent spectrum of the magnetic NS atmosphere with $B = 7 \times 10^{10}$ G and $T_{\rm eff} = 1.5$ MK (solid curve) together with emergent spectra in ordinary (O-mode, dashed curve) and extraordinary (X-mode, dotted curve) modes. *Bottom panel:* Spectra of the emergent specific intensity for the same model at different angles to the surface normal (indicated near the curves).

89°, respectively). From the comparison of the spectra at different θ we see that the angular distribution of the emergent radiation in the absorption features is different from that in the continuum. For instance, the specific intensities are more peaked towards the surface normal at energies outside the absorption features, while the radiation is generally more isotropic at the center of the features.

The bottom panels of Figures 2 and 3 show the temperature structures for the six atmosphere models. The temperature structure is only slightly affected by the relatively low magnetic fields. In particular, the magnetic field raises the temperature of upper atmospheric layers at $3 \lesssim b_{\rm eff} \lesssim 6$, apparently because of cyclotron heating, while outside of this range the surface temperature becomes lower.

4. DISCUSSION

We have presented computations of fully ionized hydrogen atmospheres of NSs for magnetic fields $B \sim 10^{10}$–10^{11} G, such that the electron cyclotron energy, $E_{c,e} \sim$ 0.1–1 keV, is within the range of energies where the thermal emission from isolated NSs is usually observed. We have shown that the peaks in the energy dependence of the free-free opacity, caused by the quantization of the electron rotation around the magnetic force lines, lead to

absorption features (quantum oscillations) at the electron cyclotron energy and its harmonics in the atmosphere spectra. The quantum oscillations are best observable at moderately large values of the quantization parameter, $0.5 \lesssim b_{\rm eff} \lesssim 20$, when the quantization is significant but the features are not too far in the Wien tail of the spectrum. The equivalent widths of the absorption features reach $\sim$ 100–200 eV in the examples considered; they grow with increasing $b_{\rm eff}$ and are lower for higher harmonics.

At least two absorption features, at energies 0.7 and 1.4 keV, with equivalent widths $\sim$ 100 eV have been observed in the X-ray spectrum of the CCO 1E 1207 (Sanwal et al. 2002). Since the thermal and cyclotron energies are essentially nonrelativistic for this object ($kT_{\rm eff}/m_e c^2 < E_{c,e}/m_e c^2 \sim 10^{-3}$), the features cannot be explained as due to the commonly known cyclotron processes. On the other hand, as $b_{\rm eff} \sim 3$–5, the features can be naturally interpreted as caused by the quantum oscillations. We note that our calculations support the reality of the suspected features at 2.1 and 2.8 keV in the 1E 1207 spectrum (Bignami et al. 2003). To confirm our interpretation and infer the properties of the 1E 1207's atmosphere, the phase-dependent spectra of 1E 1207 should be compared with the model spectra obtained by integrating the specific intensities over the visible NS surface at different rotation phases, for various orientations of the rotation and magnetic axes.

In addition to 1E 1207, there exist other NSs with similar magnetic fields and temperatures whose emission can be described by our atmosphere models. In particular, other CCOs, which likely have magnetic fields $\sim 10^{10}$–10^{11} G (Halpern & Gotthelf 2010, and references therein), are expected to show quantum oscillations in their soft X-ray spectra. However, conditions for their observation may be less favorable. For example, for the spin-down magnetic field $B_{\rm sd} = 3.1 \times 10^{10}$ G of the CCO J1852+0040 in the Kesteven 79 SNR (Halpern & Gotthelf 2010), the spectrum should show absorption features at the cyclotron energy, $E_{c,e}^\infty = 0.36(1 + z)^{-1}$ keV and its harmonics. However, as the spectrum below ~ 1 keV is strongly absorbed by the ISM ($N_{\rm H} \approx 1.8 \times 10^{22}$ cm^{-2}), only high harmonics, whose equivalent widths are small, might be detectable. Interestingly, the spectrum of this CCO, detected by the *XMM-Newton* EPIC detectors (see Figure 3 in Halpern & Gotthelf 2010), shows a hint of an absorption feature at $E \simeq 1.3$ keV, which might be third or fourth harmonic of the cyclotron energy, $E_{c,e}^\infty \approx 0.33$ or 0.26 keV, respectively[7]. To confirm the feature and estimate the cyclotron energy and gravitational redshift, a deeper observation of this CCO is required.

For the other pulsating CCO, J0822–4300 in the Puppis A SNR, the period derivative has not yet been measured, and only an upper limit on the magnetic field, $B_{\rm sd} < 9.8 \times 10^{11}$ G, has been estimated by Gotthelf & Halpern (2009). Fitting the spectrum with a double blackbody model, these authors found an emission feature around 0.8 keV at some phases. To explain the fact

---

[7] Halpern & Gotthelf (2010) do not mention this feature. We note that it is seen in the EPIC pn and MOS spectra, which supports the reality of this feature despite its low statistical significance in each of the spectra.

that the feature is seen in emission, one has to assume an energy source in the upper layers of the atmosphere, such as the heat released by accreting matter, which is not included in our models. However, it seems that the spectral structure at these energies (see Figure 3 in Gotthelf & Halpern 2009) can also be interpreted as an absorption feature, perhaps a cyclotron line, centered at ≈ 0.9 keV, which of course would imply a different continuum. To examine this interpretation and look for quantum oscillations, the CCO's phase-resolved spectra should be fitted with our atmosphere models.

Another class of NSs with possible quantum oscillations in their spectra are radio pulsars with magnetic fields 10^{10}–10^{11} G. There are 62 pulsars with such fields in the ATNF Pulsar Catalogue[8], but none of them has been observed in X-rays. As these pulsars are old (the youngest one, PSR J1810–1820 with $B_{sd} = 4.3 \times 10^{10}$ G, has the spin-down age $\tau_{sd} = P/2\dot{P} = 47$ Myr), the bulk of NS surface is too cold to be seen in X-rays, but their polar caps can be heated up to ~ 1–3 MK by relativistic particles and γ-rays generated in the pulsar magnetosphere (see, e.g., Zavlin & Pavlov 2004). Observing the quantum oscillations in the thermal spectra of polar caps is, however, a challenging task because the luminosity of this component is low and it is strongly absorbed by the ISM for many of the pulsars.

In conclusion, we should mention that the opacities by PP76, used in our atmosphere models, become inaccurate close to the centers of the quantum peaks, especially at the core of the fundamental cyclotron line. A more accurate consideration, which would include corrections to the Born approximation and the collective (high-density) effects (e.g., Sawyer 2007), and take into account the Doppler broadening of the fundamental resonance (Pavlov et al. 1980a), should broaden the spectral features and decrease the number of observable ones. Also, it would be worthwhile to investigate the role of the relativistic corrections to the opacities (including the resonances at the cyclotron harmonics). Finally, for the comparison with the observational data, it would be useful to construct atmosphere models with magnetic fields inclined to the normal to the surface and integrate the emission over (a fraction of) the NS surface. We plan to consider these problems in future works.

REFERENCES

Bignami, C. F., Caraveo, P. A., De Luca, A., & Mereghetti, S. 2003, Nature, 423, 725
De Luca, A. 2008, in AIP Conf. Proc. 983, 40 Years of Pulsars: Millisecond Pulsars, Magnetars and More, ed. C. Bassa et al. (Melville, NY: AIP), 311
Ginzburg, V. L. 1970, The Propagation of Electromagnetic Waves in Plasmas (Oxford: Pergamon)
Gnedin, Yu. N., & Pavlov, G. G. 1974, Sov. Phys. JETP, 38, 903
Gotthelf, E. V., & Halpern, J. P. 2009, ApJ, 695, L35
Halpern, J. P., & Gotthelf, E. F. 2010, ApJ, 709, 436
Kaminker, A. D., Pavlov, G. G., & Shibanov, Yu. A. 1982, Ap&SS, 86, 249
Kaminker, A. D., Pavlov, G. G., & Shibanov, Yu. A. 1983, Ap&SS, 91, 167
Manchester, R. N., Hobbs, G. B., Teoh, A., & Hobbs, M. 2005, AJ, 129, 1993
Nagel, W. 1980, ApJ, 236, 904
Pavlov, G. G., & Panov, A. N. 1976, Sov. Phys. JETP, 44, 300 (PP76)
Pavlov, G. G., & Shibanov, Yu. A. 1978, Sov. Astr., 22, 214
Pavlov, G. G., Mitrofanov, I. G., & Shibanov, Yu. A. 1980a, Ap&SS, 73, 63
Pavlov, G. G., Shibanov, Yu. A., & Yakovlev, D. G. 1980b, Ap&SS, 73, 33
Pavlov, G. G., Shibanov, Yu. A., Zavlin, V. E., & Meyer, R. D. 1995, in The Lives of the Neutron Stars, eds. M. A. Alpar, Ü. Kiziloğlu, & J. van Paradijs (Kluwer: Dordrecht), 71
Pavlov, G. G., Sanwal, D., Garmire, G. P., & Zavlin, V. E. 2002, in ASP Conf. Ser. 271, Neutron Stars in Supernova Remnants, ed. P. O. Slane & B. Gaensler (San Francisco, CA: ASP), 247
Pavlov, G. G., Sanwal, D., & Teter, M. A. 2004, In IAU Symp. 218, Young Neutron Stars and Their Enviroments, ed. F. Camilo & B. Gaensler (San Francisco, CA: ASP), 239
Pottschmidt, K., et al. 2005, ApJ, 634, L97
Sanwal, D., Pavlov, G. G., Zavlin, V. E., & Teter, M. A. 2002, ApJ, 574, L61
Sawyer, R. F. 2007, arXiv:0708.3049
Shibanov, Yu. A., Zavlin, V. E., Pavlov, G. G., & Ventura, J. 1992, A&A, 266, 313
Suleimanov, V. F., Potekhin, A. Y., & Werner, K. 2009, A&A, 500, 891
van Adelsberg, M., & Lai, D. 2006, MNRAS, 373, 1495
Zavlin, V. E., Pavlov, G. G., & Trümper, J. 1998, A&A, 331, 821
Zavlin, V. E., Pavlov, G. G., Sanwal, D., & Trümper, J. 2000, ApJ, 540, L25
Zavlin, V. E., & Pavlov, G. G. 2004, ApJ, 616, 452

Gotthelf, E. V., & Halpern, J. P. 2007, ApJ, 664, L35

[8] See http://www.atnf.csiro.au/research/pulsar/psrcat and Manchester et al. (2005).